Optical Coupling Between a Self-Assembled Microsphere Grating and a Rib Waveguide

Chao-Yi Tai, Bayram Unal, James S. Wilkinson

Optoelectronics Research Centre, University of Southampton, Highfield, Southampton,SO17 1BJ, United Kingdom

cyt@orc.soton.ac.uk

Mohamed A. Ghanem and Philip N. Bartlett

School of Chemistry, University of Southampton, Highfield, Southampton, SO17 1BJ, United Kingdom

We report the fabrication of a linear array of self-assembled polystyrene microspheres side-coupled to a rib waveguide. The optical coupling between the lateral evanescent field and the periodically perturbed effective refractive index alongside the waveguide results in a transmission stopband at the Bragg wavelength. The observed transmission spectrum shows a notch centered at $\lambda \approx 1590$nm, which is in close agreement with theory. The coupling coefficient, κ, and the spectral response are derived for variable cladding medium index using perturbation theory. Structures of this type are expected to find application in wavelength selection, optical sensing, and optical delays.

There is growing interest in integrating more functionality in planar lightwave circuits (PLCs). Wavelength selective devices are in particularly high demand due to their ability to provide filtering, routing and feedback, which are fundamental requirements for signal processing. Bragg gratings realised in planar waveguides date back to the early 1970's[1] and intensive research on distributed feedback structures has been pursued since then. Photosensitive[2,3] and etched relief gratings[4,5] are presently the most widely used structures. In comparison, relief gratings provide greater material flexibility because there is no requirement for photosensitivity. However, sub-micron scaled patterning and stringent etching tolerances are unavoidable for transferring patterns onto waveguides, resulting in high fabrication costs.

Recently, with processing techniques for producing mono-dispersed spherical colloids becoming mature, considerable research has been devoted to self-assembled photonic structures. Based on this simple and inexpensive technique, 3D photonic crystals have been fabricated.[6,7] Using a patterned substrate as a template, self-assembly has been tailored to fabricate more complex and well-defined structures.[8,9]

In this letter, we demonstrate a self-assembled microsphere grating hybridised with a rib waveguide. Sub-micron polystyrene spheres (n_p =1.59) were self-assembled to one side of a photolithographically-defined rib waveguide, forming a linear array. As

the spheres are placed against the waveguide, the optical field is drawn out resulting in a strengthened interaction with the spheres. The resultant periodic perturbation of the refractive index experienced by the modal evanescent field leads to coupling to the backward-travelling mode at the Bragg wavelength. The waveguide was designed to be single mode at the wavelength of operation, to be sufficiently narrow to ensure that a significant proportion of the modal power travelled in the lateral evanescent region, and to have a sufficient height to trap the microspheres physically. A 500nm thick layer of tantalum pentoxide (Ta_2O_5, $n \approx 2$) was first sputtered from a Ta_2O_5 target in an Ar/O_2 (16/6 sccm, 35 mTorr) atmosphere onto a Si wafer with a 2μm thick SiO_2 buffer layer, with the substrate held at 250°C. The film was then photolithographically patterned with stripes of photoresist of nominal width 1 μm, and argon ion beam milled to transfer the pattern into the Ta_2O_5 resulting in a rib waveguide with an etch depth of 500 nm, and a width of approximately 1 μm.

In preliminary work, microspheres were assembled on both sides of the waveguide, but this led to degradation in the effective strength of the grating due to misalignment between the two sides. To avoid this problem, we intentionally assembled polystyrene spheres along only one side of the rib waveguide by first coating photoresist over one side of the waveguide. A fluidic cell was then assembled by sandwiching a gasket (~0.5 mm thick) between the waveguide substrate and a cover glass. A suspension of

mono-dispersed polystyrene spheres (1wt%, 499±5 nm in diameter, Brookhaven Ltd.) was then injected into the cell with a syringe. The sample was then placed vertically in a temperature-controlled (25°C) incubator to allow controlled evaporation, causing the liquid meniscus to draw the polystyrene spheres across the sample at a speed of 1.5 mm/h during the dewetting process, as shown in Fig. 1(a). Once the spheres were physically trapped by the rib waveguide, the capillary immersion force[10] forced the beads to adjust themselves into a well-packed array lined up along the waveguide. When the cell had dried, the sample was heated to 93°C for 1 minute in order to stick the polystyrene spheres to the surface of the waveguide. The remaining photoresist was then removed using 2-propanol, thereby lifting the microspheres away from on one side of the rib. A microsphere array of approximately 3mm length was formed along the waveguide. A scanning electron micrograph of part of the resultant device is shown in Fig. 1(b).

Figure 1(c) shows the transmission spectra (TE polarized) for different cladding media, normalised to those obtained in the absence of spheres. When the device was surrounded by air, the transmission spectrum shows a notch centred at λ=1591 nm with a depth of approximately 1.47 dB (28%) and a bandwidth at full width at half maximum power ($\delta\lambda_{FWHM}$) of 17 nm. As the refractive index of the cladding medium increases to n=1.71 (index matching oil), the centre of the stopband shifts to a longer

wavelength of λ=1679 nm and exhibits a greater depth of 2.1 dB (38%) and a bandwidth $\delta\lambda_{FWHM}$ of 11nm.

To explain the observed spectra, we applied perturbation theory[11] to the composite system shown in Fig. 2(a). The refractive index profile along the waveguide in the presence of the linear array of spheres can be represented by:

$$N(z) = N_{eff} + \eta(z)\Delta n \tag{1}$$

where N_{eff} is the effective refractive index of the waveguide, $\Delta n = n_p - n_{clad}$ is the amplitude of perturbation, and η is the overlap integral between the evanescent field and the polystyrene sphere at position z, defined by:

$$\eta(z) = \frac{\beta}{2\omega\mu} \int_{x1(z)}^{x2(z)} E_y^{\,2}(x)dx \tag{2}$$

where $\beta = N_{eff}k$, and $k = 2\pi/\lambda$ is the propagation constant in vacuum. The evanescent field decays exponentially into the cladding medium with the form of:

$$E_y(x) = E_0 \exp(-x/d) \tag{3}$$

where E_0 represents the field strength on waveguide surface and $d = (\lambda/2\pi)(N_{eff}^2 - n_{clad}^2)^{-1/2}$ is the penetration depth. Substituting (3) in (2), the magnitude of perturbation can be derived:

$$\eta(z)\Delta n = \frac{\beta}{2\omega\mu}(E_0)^2 d \exp(-\frac{2a_0}{d}) Sinh\left[\frac{2a_0}{d}\sqrt{1-(\frac{z}{a_0})^2}\right]\Delta n \tag{4}$$

Fig. 2(b) plots the periodically perturbed refractive index alongside the waveguide. As the index profile is an even function with respect to z=0, it can be expressed as a Fourier series:

$$\eta(z)\Delta n = \Delta n_0 + \sum_{m=1}^{s} \Delta n_m \cos\frac{m\pi}{a_0} z \qquad (5)$$

The DC term Δn_0 contributes to the effective refractive index N_{eff}, causing the shift of Bragg wavelength. The reflection wavelength is then given by $\lambda_{Bragg} = 2(N_{eff}+\Delta n_0)\Lambda$, where Λ is the grating period. The value of N_{eff} for the Ta_2O_5 rib waveguide here is determined by the finite-difference beam propagation method, assuming Ta_2O_5 has an index of 2.0. The grating period, Λ, estimated from the digitised SEM image with a resolution of 13 nm/pixel, is 493±9 nm. The Bragg reflection wavelength is calculated and plotted as a function of cladding index in Fig. 3, with error bars indicating the effect of specified deviations in the particle size and the uncertainty in N_{eff}. The experimental data points are within the error bars showing agreement with theory. The strength of grating may be described by the coupling coefficient, which is defined as $\kappa=(\pi\Delta n/\lambda_{Bragg})\eta$.[12] Fig. 3 shows the numerically-determined coupling coefficient as a function of cladding index. From this diagram it is expected that, as the cladding index increases from unity, the strength of the interaction first increases slightly. Then, as the cladding index approaches that of the spheres, n_p=1.59, the reduced

sphere/cladding index contrast becomes more significant than the increasing overlap between the evanescent field and the spheres, and the coupling coefficient falls. When the cladding index becomes larger than n_p=1.59, the coupling coefficient rises rapidly, due to a combination of increasing index contrast and extending field. In the experiment presented here, the deeper transmission notch at the Bragg wavelength in the case of the oil cladding demonstrates this behaviour. The transmission drop, enhanced by a factor of 1.38 (from 28% to 38%), agrees well with the enhanced coupling coefficient ($\kappa_{oil}/\kappa_{air}$=1.35). The bandwidths of the spectral notches are much greater than would be expected from a weak uniform grating of 3mm length. However, this is a randomly perturbed periodic system,[13,14] and the deviation in the diameters of the spheres, imperfections in the periodicity of the packing and imperfections in the rib waveguide will contribute to this broadening and will also cause a reduction in the depth of the transmission notch. It is expected that with improved sphere diameter control and more uniform assembly, a deeper and narrower response will be achieved.

In conclusion, we have demonstrated a side-coupled rib waveguide microsphere grating using a simple low-cost self-assembly process. The optical coupling between the lateral evanescent field and the self-assembled array results in a stopband in the transmission spectrum, at a wavelength of $\lambda \approx 1590$nm, in close agreement with theory. Grating strength adjustment has been examined by varying the refractive index of the

overlaid cladding medium, and an extinction of 38% has been obtained. This study demonstrates the potential for self-assembly of microspheres with waveguides for wavelength-dependent devices, and it is expected that this may be extended to microspheres and microsphere resonators of other materials or as part of more sophisticated planar lightwave circuit configurations.

References

[1]D. C. Flanders, H. Kogelnik, R. V. Schmidt, and C. V. Shank, *Appl. Phys. Lett.* **24**, 194 (1974).

[2]M. Ibsen, J. Hubner, J. E. Pedersen, R. Kromann, L. –U. A. Andersen, and M. Kristensen, *Electron. Lett.* **35**, 585 (1996).

[3]D. F. Geragthy, D. Provenzano, W. K. Marshall, S. Honkanen, A. Yariv, and N. Peyghambarian, *Electron. Lett.* **35**, 585 (1999).

[4]J. E. Román and K. A. Winick, *Appl. Phys. Lett.* **61**, 2744 (1992).

[5]R. Adar, C. H. Henry, R. C. Kistler, and R. F. Kazarinov, *Appl. Phys. Lett.* **60**, 1779 (1992).

[6]I. I. Tarhan, and G. H. Watson, *Phys. Rev. Lett.* **76**, 315 (1996).

[7]Y. A. Vlasov, X. Z. Bo, J. C. Sturm, and D. J. Norris, *Nature*, **414**, 289 (2001).

[8]Y. –H. Ye, S. Badilescu, Vo-Van Truong, P. Rochon, and A. Natansohn, *Appl. Phys. Lett.* **79**, 872 (2001).

[9]Y. Yin, Yu Lu, B. Gates, and Y. Xia, *J. Am. Chem. Soc.* **123**, 8718 (2001).

[10]N. D. Denkov, O. D. Velev, P. A. Kralchevsky, I. B. Ivanov, H. Yoshimura, and K. Nagayama, Langmuir, **8**, 3183 (1992).

[11]A. W. Snyder and J. D. Love, *Optical Waveguide Theory*, (Chapman and Hall,

London, 1983).

[12]I. Bennion, J. A. R. Williams, L. Zhang, K. Sugden, and N. J. Doran, *Opt. Quantum. Electron.*, **28**, 93 (1996).

[13]J. M. Frigerio, J. Rivory, and P. Sheng, *Opt. Comm.* **98**, 231 (1993).

[14]D. Zhang, Z. Li, W. Hu, and B. Cheng, *Appl. Phys. Lett.* **67**, 2431 (1995).

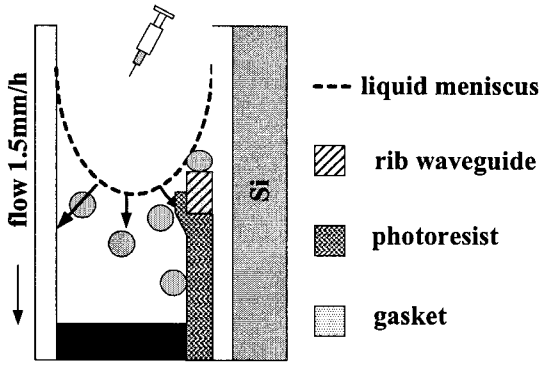

(a)

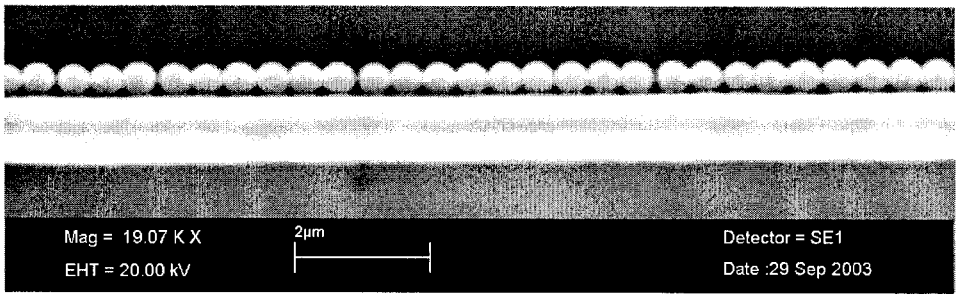

(b)

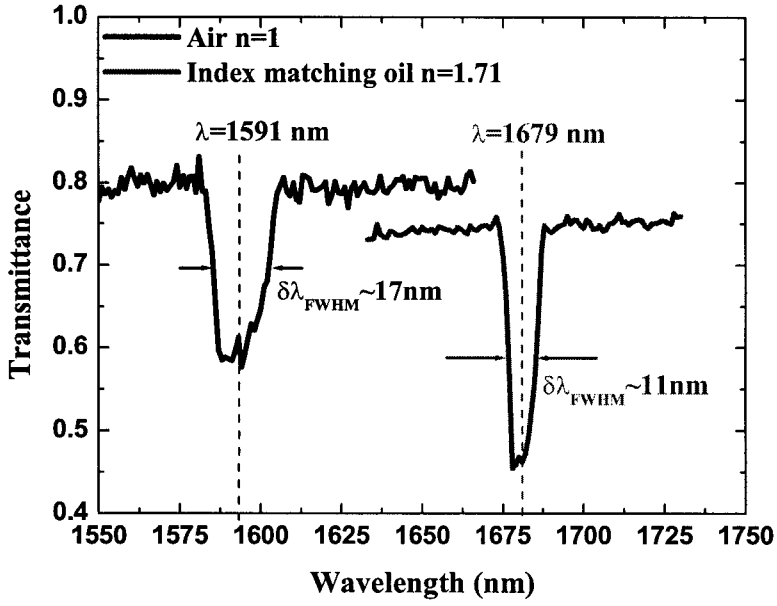

(c)

Fig. 1(a) Schematic diagram of the self-assembly procedure.

Fig. 1(b) SEM image of the rib waveguide with self-assembled array.

Fig. 1(c) Transmission spectra for cladding media of index 1.0 and 1.71.

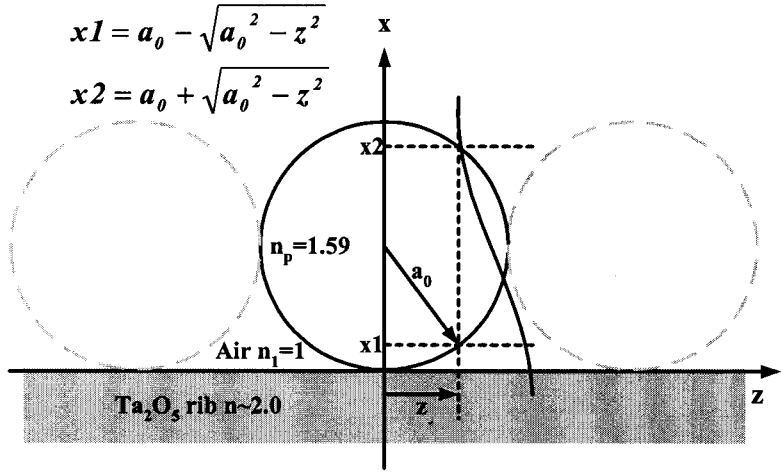

(a)

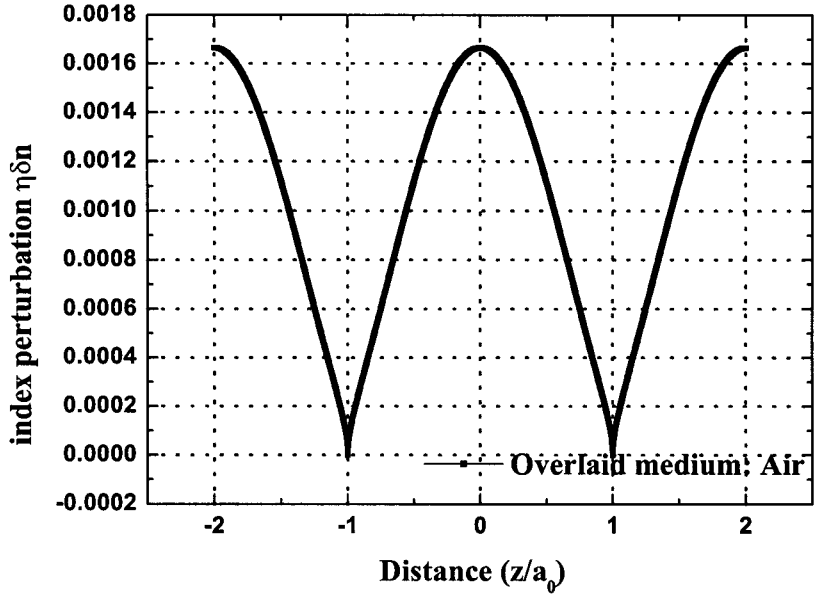

(b)

Fig. 2(a) Configuration of the microsphere grating side-coupled to the rib waveguide.

(b) Calculated effective index perturbation along the waveguide.

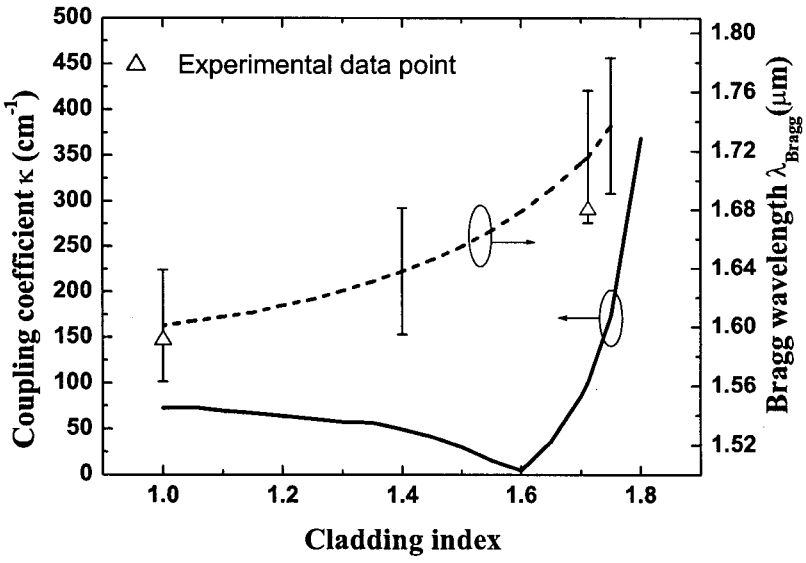

Fig. 3. Calculated coupling coefficient and Bragg wavelength as a function of cladding refractive index.